Dynamic Acoustic Field for Tuneable and Scalable Particle Sorting

Dynamic Acoustic Field for Tuneable and Scalable Particle Sorting

G.D. Skotis[1], M.A.B. Andrade[2], S. Ritchie[1], D.R.S. Cumming[1], M.O. Riehle[3], A.L. Bernassau*[4]

[1]School of Engineering, University of Glasgow, UK
[2]Institute of Physics, University of São Paulo, Brazil
[3]Institute of Molecular, Cell and Systems Biology, University of Glasgow, UK
[4]School of Engineering and Physical Sciences, Herriot-Watt University, UK

Abstract— **Separation of cells is a critical process for studying cell properties, disease diagnostics, and therapeutics. Cell sorting by acoustic waves offers a means to separate cells on the basis of their size and physical properties in a label-free, contactless, and biocompatible manner. In this work, we introduce a unique technique, which use a dynamic acoustic field (DAF), based on the modulation of the phase of the standing wave. Using our dynamic acoustic field, we successfully separated 10 and 45 µm diameter polystyrene particles with a separation efficiency of 100%, and separated 6 and 10 µm polystyrene particles with an efficiency of ~97%. We illustrate that DAF is capable of effectively separating dorsal root ganglion cells from heterogeneous medium. Finally, we demonstrate the scalability of the DAF method by sorting polystyrene particles of 5 mm and 2 mm diameter in air.**

Keywords— Acoustic radiation pressure; acoustic particle sorting; acoustic particle manipulation.

I. INTRODUCTION

Many applications in biology and medicine call for efficient and reliable separation of particles and cells for disease diagnosis, genetic analysis, drug screening, and therapeutics. Nowadays, numerous methods are available to separate and sort cells, such as magnetic [1], dielectric [2], optical [3] and acoustic [4] methods. Among these methods, acoustic manipulation techniques have the advantage of working with any material [4]. Acoustic manipulation and separation methods of cells and other biological materials can be performed by using both static [5], [6] and dynamic [7], [8] standing wave fields.

In this paper, we demonstrate a flow-less dynamic acoustic field (DAF) method that can be used to separate particles depending on their size within a sample volume. We also study the discriminative ability of the method for particles of different sizes by separating an heterogeneous mixture of 10 and 45 µm diameter polystyrene particles and then 6 and 10µm polystyrene particles. We illustrate the effectiveness of the DAF technique for biological–biomedical applications by sorting primary pig dorsal root ganglion neurons as a contact-less means of separating these neurons from debris and smaller cells, which results from tissue digestion. Finally, we demonstrate the scalability of the DAF method, by sorting polystyrene particle of 5 mm and 2 mm diameter in air.

It has been demonstrated that one transducer and a reflector can be used to create a standing wave that traps particles. With this technology, it was possible to trap particles and transport them by changing the driving frequency [9], [10]. This method presents several challenges, such as an unstable force resulting in movement among trapped particles. An alternative method is to form interference patterns using traveling acoustic waves. Courtney *et al.* [11] describe a device in which acoustically matched transducers are used in opposed pairs. In this arrangement, sound emitted by a given transducer is absorbed by its opposing transducer.

Acoustic sorting is based on two sound waves traveling in opposite directions which create a standing wave with maxima and minima of acoustic energy. When particles are dispersed in the medium through which the standing wave propagates, they can be manipulated based upon their mechanical properties such as size, density or compressibility. The particles can be manipulated by changing the phase of one of the opposite transducers.

II. METHOD

The DAF technique is based on the time variant primary acoustic force, F_a (1), combined with the viscous force, F_v (3) enabling discrimination of particles according to their physico-mechanical properties. The acoustic force is dependent on the particle radius and particle density. Smaller or less dense particles and cells experience a lower acoustic force F_a, with respect to larger or denser particles and cells; therefore, particles and cells of different sizes and different densities will separate.

The DAF method relies on an interplay between acoustic radiation forces and viscous drag forces. The primary acoustic radiation force F_a that acts on a small particle in a plane standing wave is given by [6]

$$F_a = -\left(\frac{\pi p_0^2 V_c \beta_w}{2\lambda}\right) \times \phi(\beta,\rho) \times \sin(2kx)\,, \qquad (1)$$

where p_0 is the acoustic pressure amplitude, V_c is the volume of the particle, λ is the wavelength, $k = 2\pi/\lambda$ is the wave number, x is the distance from a pressure node, and $\phi(\beta,\rho)$ is the acoustic contrast factor, given by

$$\phi(\beta,\rho) = \frac{5\rho_c - 2\rho_w}{2\rho_c + \rho_w} - \frac{\beta_c}{\beta_w}\,. \qquad (2)$$

Part of this work was supported by an EPSRC EFutures grant (RES/0560/7386) and a Royal Society Research grant (RG130493). Support from GU68 Engineers Trust of the United Kingdom and São Paulo Research Foundation - FAPESP (grant #2014/24159-1) are gratefully acknowledged.

The acoustic contrast factor ϕ depends on both the particle density ρ_c and its compressibility β_c in relation to the corresponding properties of the surrounding medium (ρ_w, β_w). The equation of the primary radiation force, F_a, (1), states that the acoustic force applied on the particles is proportional to the acoustic pressure amplitude p_0 squared and to the volume of the particles V_c.

The viscous force F_v that acts on a spherical particle is given by the Stokes drag equation:

$$F_v = -6\pi\eta R v\,, \tag{3}$$

where η is the medium viscosity, R is the particle radius, and v is the relative velocity between the particle and the fluid.

The DAF technique relies on a repeated cycling pattern of the phase difference between two excited transducers from 0° to 360°. Within each cycle, the phase is swept completely through 360° over a time t_{ramp} and then allowed to rest for a period t_{rest} before commencing the next cycle. The interplay between the rate at which the phase is swept and the length of the rest time is at the core of the separation technique.

During t_{ramp}, under the correct conditions, the larger particles experience a strong acoustic force compared to the viscous force, and move with the acoustic field. The smaller particles are under the influence of the viscous force and thus are not affected by the acoustic field and stay in their initial position. Figure 1(a) illustrates the cycling of the swept phase and Fig. 1(b) the movement of large and small particles with time.

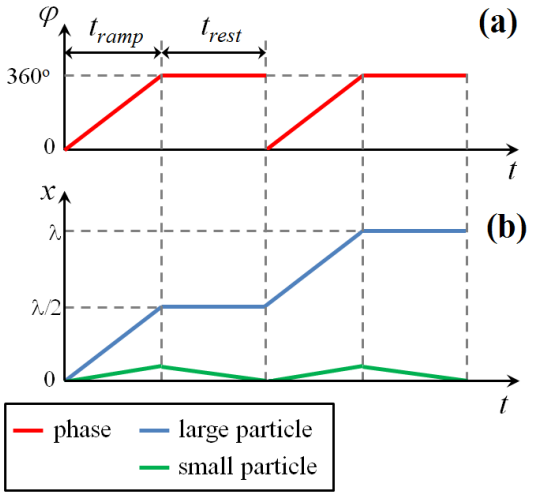

Figure 1. (a) Cycle of the swept phase from 0° to 360°. (b) The effect of the applied phase shift on large and small particles. The large particles move with greater velocity than small particles, thus when the phase shift reaches the rest period at 360° the large particles continue forward and reach the next acoustic node and are trapped. However, the small particles relax back to the initial node.

III. Results and Discussion

A. Dynamic Acoustic Field in Liquid

The acoustic device, described elsewhere [12] has been used to demonstrate how the dynamic acoustic field technology can be applied to particle sorting. In this setup configuration, only two opposite transducers were used. Synchronization between the two channels was achieved using two linked arbitrary waveform generators providing four output channels each (TGA12104, Aim and Thurlby Thandar Instruments, UK) allowing independent control of the amplitude, phase and frequency of each channel. The signals from the waveform generators were amplified and electronically matched by high speed buffers (BUF634T, Texas Instruments, USA). The system is controlled by a virtual control panel developed in Labview (National Instruments, UK), which allows real time voltage, frequency and phase control. The interface allows interactive and precise positioning and manipulation of the micro particles. Furthermore, an agar layer was introduced into the device to minimize the streaming [13] and maximize the precision in control of the particle movement.

The separation experiments were conducted using two mixtures of particles, each at a particle density of 4.99 × 10^5 particles mL^{-1}. Mixture A contained 10 and 45 µm diameter particles at a ratio of 1 : 100. Mixture B contained 6 and 10 µm diameter particles at a ratio of 1 : 100. At these concentrations, no aggregation of particles was observed.

Figure 2(a) shows the particle separation for the mixture A. The 45 µm diameter particles follow the shifted acoustic field (moving towards the right-hand side), while the 10 µm diameter particles stay close to the position of the original node. The time between frames was 0.5 s. It was found that 100% of particles separate, with an efficiency and a purity of 100%. These results were achieved with a value of t_{ramp} = 8 s and t_{rest} = 4 s.

The experiments were replicated, with the mixture B, using 6 and 10 µm diameter particles. For these particles, it was found that ~97% of particles separate, with an efficiency and a purity of ~97%. These results were achieved with a value of tramp = 15 s and t_{rest} = 15 s. Figure 2(b) shows the average movement of the 6 and 10 µm particles under the DAF separation. The 10 µm diameter particles move from node to node (moving towards the right-hand side), while the smaller particles (6 µm in diameter) remain close to their initial position of the original node.

To assess the technique for biological–biomedical applications, we applied the DAF to separate porcine dorsal root ganglion (DRG) neurons from a freshly isolated mixture containing myelin debris and other non-neuronal cells. The DRG neurons have an average size from 17 to 145 µm, while the myelin debris has a size of approximately from 10 to 15 µm.

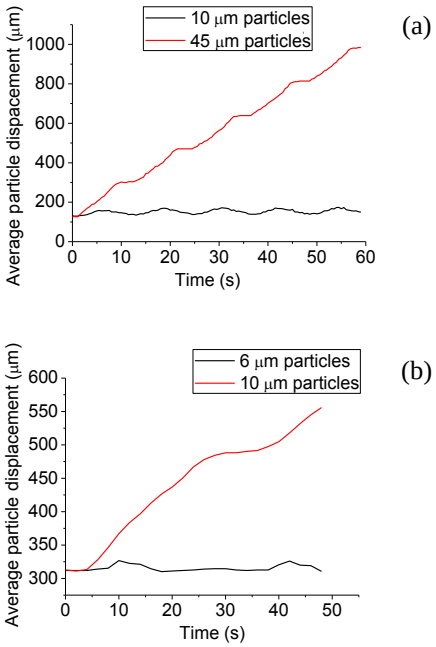

Figure 2 (Color online) Graph showing the average displacement with time (a) for the mixture A containing 45 and 10 μm particles, (b) for the mixture B containing 10 and 6 μm particles.

A dynamic acoustic field was then applied (using a t_{ramp} = 5 s and t_{rest} = 5 s), and the average displacement of cells with time is represented in Figure 3. The static material (myelin debris and non-neuronal cells) does not produce a trace, whereas the DRG cells shows a trace that moves from left to right. The DRG cells follow the shifted acoustic field (moving towards the right-hand side), while the debris exhibits minimal displacement of the original node.

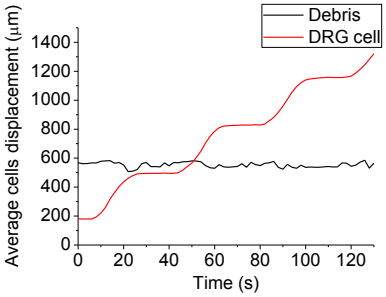

Figure 3 (Color online). Graph showing the average displacement of cells with time. The red trace represents the displacement of the DRG, moving from node to node while the debris (black trace) is staying in place.

B. Dynamic Acoustic Field in Air

To demonstrate the scalability of the DAF sorting technique, we now investigate sorting in air. The acoustic system, Figure 4, is formed by two speakerphones (BMS 4550 model, Germany) mounted into a frame allowing accurate control of the spacing. A 7 mm thickness glass plate is positioned horizontally between the speakerphones with its upper surface coinciding with the main axes of the speakers' diaphragms. The acoustic standing wave was produced by exciting both speakers with sinusoidal waves at a frequency of 17.5 kHz.

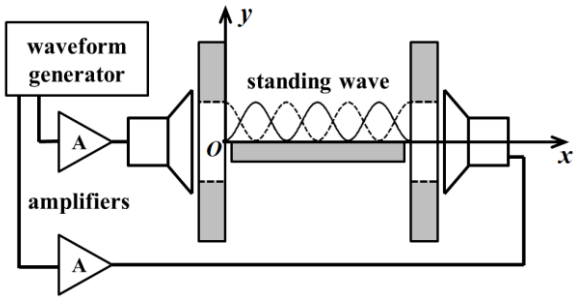

Figure 4. Acoustic system formed by two speakerphones.

To demonstrate the sorting technique 2 mm and 5 mm expanded polystyrene particles were placed on the glass plate and the DAF cycling pattern (Figure 1) was repeated three times, with t_{ramp} = 0.7 s and t_{rest} = 1.3 s.

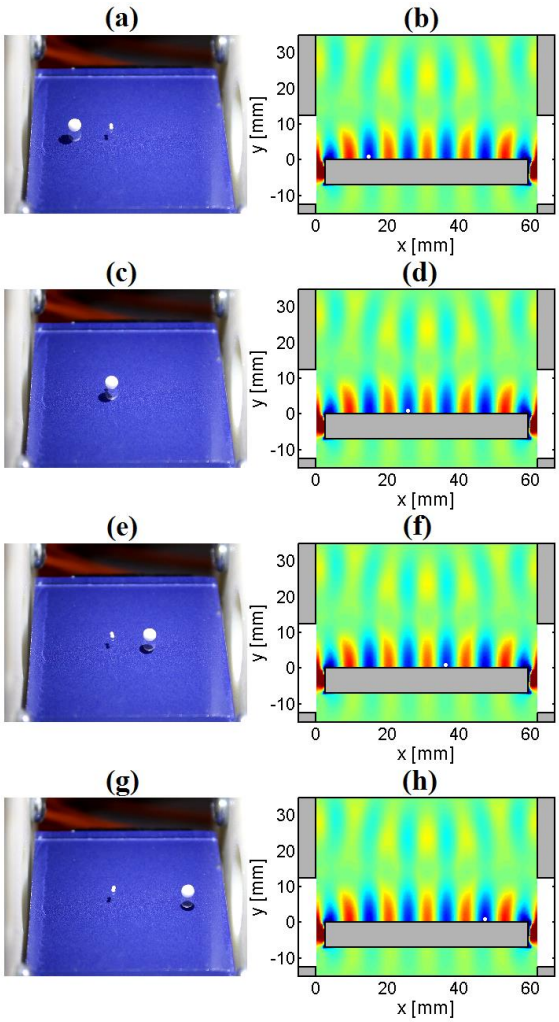

Figure. 5 (Color Online). Photograph of particle position (left hand side) and simulation (right hand side) of the node displacement related to the particle motion.

Figure 5 shows the evolution of the particle movement under the DAF. Initially, the large particle is located at the second potential well (x = 14.8 mm) and the small particle is located at the third one (x = 25.8 mm). After three cycles, the large particle is transported from the second to the fifth potential well (x = 47.2 mm), while the small particle remains at the third potential well. The large expanded polystyrene particle, experiencing a larger acoustic force, moves during t_{ramp} and stabilizes during t_{rest} at the next node, resulting in an overall displacement over time. Simultaneously, the small expanded polystyrene particle, experiencing lower acoustic force, and move only slightly, returning to the initial node position during t_{rest}. We investigated several parameters of t_{ramp} and t_{rest} and identified that for t_{ramp} = 0.7 s with t_{rest} = 1.3 s, particles of 5 mm diameter where transported whilst 2 mm diameter particles remained in place. Figure 5 shows the particle displacement (experimental data) related to the node displacement (simulation). It can be seems that there is a good agreement between the simulation and experimental data.

IV. CONCLUSION

We first demonstrate the method for the separation of particles with different diameters between 6 and 45 μm in a heterogeneous medium. The dynamic acoustic field is then used to separate dorsal root ganglion cells. The shearless, label-free and low damage characteristics make this method of manipulation particularly suited for biological applications. Advantages of using a dynamic acoustic field for the separation of cells include its inherent safety and biocompatibility, the possibility to operate over large distances (centimeters), high purity (ratio of particle population, up to 100%), and high efficiency (ratio of separated particles over total number of particles to separate, up to 100%). The DAF method has also proved to be scalable and capable of sorting polystyrene particles of 5 mm and 2 mm diameter in mid-air.

REFERENCES

[1] K.E. McCloskey, J.J. Chalmers, and M. Zborowski, "Magnetic cell separation: characterization of magnetophoretic mobility", Anal. Chem., vol. 75, pp. 6868-6874, 2003.

[2] R. Pethig, "Dielectrophoresis: status of the theory, technology, and applications", Biomicrofluidics, vol. 4, art. no. 022811, 2010.

[3] V. Marx, "Biophysics: using sound to move cells", Nat. Methods, vol. 12, pp. 41-44, 2015.

[4] D.G. Grier, "A revolution in optical manipulation", Nature, vol. 424, pp. 810-816, 2015.

[5] F. Petersson, A. Nilsson, C. Holm, H. Jönsson, and T. Laurell, "Separation of lipids from blood utilizing ultrasonic standing wave fields in microfluidic channels", Analyst, vol. 129, pp. 938-943, 2004.

[6] T. Laurell, F. Petersson, and A. Nilsson, "Chip integrated strategies for acoustic separation and manipulation of cells and particles", Chem. Soc. Rev., vol. 36, pp. 492-506, 2007.

[7] X. Ding, S.C.S. Lin, B. Kiraly, H. Yue, S. Li, I.K. Chiang, J. Shi, S. J. Benkovic, and T.J. Huang, "On-chip manipulation of single microparticles, cells, and organisms using surface acoustic waves", Proc. Natl. Acad. Sci. U.S.A., vol. 109, pp. 11105-11109, 2012.

[8] G.D. Skotis, D.R.S. Cumming, J.N. Roberts, M.O. Riehle, and A.L. Bernassau, "Dynamic acoustic field activated cell separation (DAFACS)", Lab. Chip, vol. 15, pp. 802-810, 2015.

[9] T. Kozuka, T. Tuziuti, H. Mitome, and T. Fukuda, "Non-contact micromanipulation using an ultrasonic standing wave field," in The Ninth Annu. Int. Workshop on Micro Electro Mechanical Systems, 1996, pp. 435‑440.

[10] P. Glynne-Jones, R.J. Boltryk, N.R. Harris, A. W. J. Cranny, and M. Hill, "Mode-switching: A new technique for electronically varying the agglomeration position in an acoustic particle manipulator," Ultrasonics, vol. 50, no. 1, pp. 68‑75, 2010.

[11] C.R.P. Courtney, C.K. Ong, B.W. Drinkwater, P.D. Wilcox, C. Demore, S. Cochran, P. Glynne-Jones, and M. Hill, "Manipulation of microparticles using phase-controllable ultrasonic standing waves," J. Acoust. Soc. Am., vol. 128, no. 4, pp. EL195‑EL199, 2010.

[12] A.L. Bernassau, C.R.P. Courtney, J. Beeley, B.W. Drinkwater, and D.R.S. Cumming, "Interative manipulation of microparticles in an octagonal sonotweezer", Appl. Phys. Lett., vol. 102, art. no. 164101, 2013.

[13] A.L. Bernassau, P. Glynne-Jones, F. Gesellchen, M. Riehle, M. Hill, and D.R.S. Cumming, "Controlling acoustic streaming in an ultrasonic heptagonal tweezers with application to cell manipulation", Ultrasonics, vol. 54, pp. 268-274, 2014.